Available online at www.sciencedirect.com
ScienceDirect
Procedia Engineering 80 (2014) 638 – 655
Procedia Engineering
www.elsevier.com/locate/procedia

3rd International Symposium on Aircraft Airworthiness, ISAA 2013

On-Line Optimization for Fault Tolerant Flight Control

Lunlong Zhong[a], Félix Mora-Camino[a]a*

[a]ENAC, MAIAA, Univ. de Toulouse, F-31055 Toulouse, France

Abstract

In this communication the case in which an aerodynamic actuator failure occurs to an aircraft while it has to perform some guidance maneuver is considered. This problem is dealt with the reassignment of remaining operational actuators in order to perform the required maneuver while maintaining the structural integrity of the aircraft. Nonlinear Inverse Control technique is used to generate online nominal moments along the three axes of the aircraft. Taking into account all material and structural constraints as well as the redundant effects from other actuators, a mathematical programming problem to be solved on-line which related to control reallocation can be formulated. Solution techniques, based on dynamic neural networks, active set methods and interior point methods are discussed and the respective performances are compared.

Selection and peer-review under responsibility of Airworthiness Technologies Research Center, Beihang University/NLAA.

Keywords: active set, interior point, neural network, on-line optimization, fault tolerant flight control

1. Introduction

In this study we consider a transportation aircraft in the situation in which a main aerodynamic actuator failure can occurs while it has to perform some guidance maneuver. Here through a nonlinear dynamic inversion (NLI) of the flight dynamics, the necessary moments to perform a given guidance maneuver are computed. It is supposed that a fault detection and identification (FDI) module is monitoring on-line the whole set of control channels and actuators. In this study it is supposed that this FDI module presents high standards of reliability, accuracy and timeliness, so its design characteristics and operations principles are not discussed in this paper. References [1-3] present up to date achievements in this area.

So when an actuator failure occurs, is detected and correctly identified, an on-line reassignment and resetting of the remaining redundant actuators must be performed with the aim of achieving anyway the

* Corresponding author. Tel.: +33-562174358, fax. +33-562174403
E-mail address: felix.mora@enac.fr.

1877-7058
Selection and peer-review under responsibility of Airworthiness Technologies Research Center, Beihang University/NLAA.
doi:10.1016/j.proeng.2014.09.119

planned maneuvers. The question is tackled here by formulating on-line optimization problem whose solution will provide continuously new reference values for these actuators, therefore allow performing the planned maneuver in a nominal or a degraded way. This represents the main difference with other previous approaches to actuator fault management [4-6].

In this study, is adopted a linear quadratic programming formulation of the optimization problem to be solved on-line since many optimization methods exist to solve it rather efficiently. Among these methods, active set methods, interior point methods and neural network dynamic solvers, described in [7-9], have been considered and compared. The main issue is to check if the performances of these techniques are compatible with their on-line operation onboard aircraft to deal with the actuator reassignment and resetting problem under failure.

2. Effectiveness of Aerodynamic Actuators

The effectiveness of the control surfaces appears through the contributions of their angular deflections to the dimensionless coefficients present in the expressions of aerodynamic forces and torques [10]. These control surfaces produce a collective external effect over the whole aircraft as well as internal efforts which should satisfy structural constraints. The global dimensionless coefficients used to express aerodynamic forces are assumed to be given by:

$$C_x = C_{x0} + k\, C_z^2 \tag{1}$$

$$C_y = C_{y\beta}\beta + C_{yp}\, pl_A/V + C_{yr}\, rl_A/V + \underline{C}_{y\delta p}'\underline{\delta}_p + \underline{C}_{y\delta r}'\underline{\delta}_r \tag{2}$$

$$C_z = C_{z0} + C_{z\alpha}\,\alpha + C_{z\delta ths}\,\delta_{ths} + \underline{C}_{z\delta q}'\underline{\delta}_q \tag{3}$$

where k is a positive coefficient and the C_{ij} are dimensionless aerodynamic derivatives, V is the airspeed, δ_{ths} is the angular position of the trimmable horizontal stabilizer and l_A is a reference length. Here p, r are respectively the roll and yaw rates, α is the angle of attack, β is the side slip angle, $\underline{\delta}_p$, $\underline{\delta}_q$, $\underline{\delta}_r$ are respectively the aileron, elevator and rudder deflections.

The dimensionless coefficients of the main axis aerodynamic torques can in general be expressed such as:

$$C_m = C_{m0} + C_{m\alpha}\,\alpha + C_{mq}\, ql_A/V + C_{m\delta ths}\,\delta_{ths} + \underline{C}_{m\delta q}'\underline{\delta}_q \tag{2.1}$$

$$C_l = C_{l0} + C_{l\beta}\beta + C_{lp}\, pl_A/V + C_{lr}\, rl_A/V + \underline{C}_{l\delta p}'\underline{\delta}_p + \underline{C}_{l\delta r}'\underline{\delta}_r \tag{2.2}$$

$$C_n = C_{n0} + C_{n\beta}\beta + C_{np}\, pl_A/V + C_{nr}\, rl_A/V + \underline{C}_{n\delta p}'\underline{\delta}_p + \underline{C}_{n\delta r}'\underline{\delta}_r \tag{2.3}$$

where q is the pitch rate. According to the relationship between aerodynamic derivatives and aerodynamic torque, the expression of the different aerodynamic torques generated by the control surfaces can be approximated by an affine form with respect to the corresponding deflections of the different aerodynamic actuators, so that we get expressions such as:

$$M_{ik}(t) = M_{ik}^0(t) + \mu_{ik}(t)\delta_k(t) \tag{3}$$

where $M_{ik}(t)$ is the i^{th} considered torques (roll, pitch, yaw, bending, flexion), $\delta_k(t)$ is the deflection of the k^{th} aerodynamic actuator ($k \in K$={aileron, flap, right spoilers, left spoilers, elevator, rudder}) and $\mu_{ik}(t)$ is the current effectiveness of actuator k to produce moment i. The current values $M_{ik}^0(t)$ and $\mu_{ik}(t)$ depend on the airspeed V, the flight level and on the values of α, β, p, q and r. Global aerodynamic torques generated by aircraft aerodynamic actuators can be rewritten in a global affine form as:

$$L(t) = L^0(t) + \sum_{i \in I^L} X_i^L(t)\ \delta_i(t) \tag{4.1}$$

$$M(t) = M^0(t) + \sum_{i \in I^M} X_i^M(t)\ \delta_i(t) \tag{4.2}$$

$$N(t) = N^0(t) + \sum_{i \in I^N} X_i^N(t)\ \delta_i(t) \tag{4.3}$$

with $I = I^L \cup I^M \cup I^N$, where I^L is the set of actuators generating some roll moment, I^N is the set of actuators generating some yaw torque, while I^M is the set of actuators generating pitch moments. Figure 1 displays, in the case of a A340 aircraft, the different aerodynamic surfaces of its wing. The current values of $L^0(t)$, $X_i^L(t)$, $M^0(t)$, $X_i^M(t)$, $N^0(t)$ and $X_i^N(t)$ depend on the airspeed V, the flight level and α, β, p, q and r.

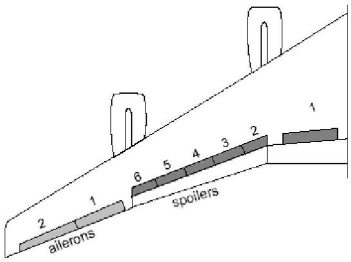

Fig. 1 Example of Wing Actuators (A340)

3. Actuators Constraints and Limitations

The deflection of each aerodynamic surface is subject to minimum and maximum bounds while its deflection rates are limited by the adopted actuator technology. Also, global physical constraints must be taken into account to ensure aircraft integrity especially when some actuators fail. These limitations should be taken explicitly into consideration by the reallocation system.

3.1. Actuators Position and Speed Limitations

With respect to control surfaces, the following bound constraints should be met:

$$\delta_i^{\min} \le \delta_i \le \delta_i^{\max} \quad i \in I \tag{5.1}$$

$$\dot{\delta}_i^{\min} \le \dot{\delta}_i \le \dot{\delta}_i^{\max} \quad i \in I \tag{5.2}$$

where $\delta_i^{\min}$, $\delta_i^{\max}$, $\dot{\delta}_i^{\min}$ and $\dot{\delta}_i^{\max}$ are the bounds and maximum deflection speed values. These conditions can be considered at sampled instants, it becomes:

$$\max\left\{\delta_i^{\min}, \delta_i(t-\Delta t) + \dot{\delta}_i^{\min}\Delta t\right\} \le \delta_i(t) \le \min\left\{\delta_i^{\max}, \delta_i(t-\Delta t) + \dot{\delta}_i^{\max}\Delta t\right\} \tag{6}$$

3.2. Global Constraints

Global constraints are in general related with structural considerations. It has been shown that total wing bending and flexion torques during maneuver can be written in an affine form as [11]:

$$M_b(t) = A_b(t) + \sum_{i \in I^{wing}} Y_{bi}(t)\, \delta_i(t) \tag{7.1}$$

and

$$M_f(t) = A_f(t) + \sum_{i \in I^{wing}} Y_{fi}(t)\, \delta_i(t) \tag{7.2}$$

with $I^{wing} \subset I$ is the set of wing actuators contributing to the bending and the flexion torques, where A_b, Y_{bi}, A_f and Y_{fi} depend on the airspeed V, the flight level and α, β, p, q and r.

Then the global wing bending and flexion constraints can be written as:

$$A_b(t) + \sum_{i \in I^{wing}} Y_{bi}(t)\; \delta_i(t) \le M_{bend}^{\max} \tag{8.1}$$

and

$$A_f\left(t\right) + \sum_{i \in I^{wing}} Y_{fi}\left(t\right)\delta_i\left(t\right) \le M_{flex}^{\max} \tag{8.2}$$

where $M_{bend}^{\max}$ and $M_{flex}^{\max}$ are maximum acceptable bending and flexion torques at the wing root. Here it is supposed that the satisfaction of these global constraints implies the satisfaction of local bending and flexion torque constraints.

To illustrate the proposed approach, here is considered the case of a pure stabilized roll maneuver where the following conditions should be met by the body angular rates of the aircraft:

$$\tau_p\; \dot{p} + p = p_c \tag{9.1}$$

$$q = 0 \tag{9.2}$$

$$\tau_r\; \dot{r} + r = (g/V)\sin\phi \tag{9.3}$$

There roll and yaw motions follow first order dynamics while pitch dynamics remains frozen. Here p_c is the desired roll rate, τ_p and τ_r are time constants. The dynamic constraint relative to the yaw rate is characteristic of a coordinated turn and its completion should allow avoiding noticeable lateral load factors during this roll maneuver.

Applying the non linear inverse control approach [12], the necessary on-line values for each aerodynamic torque are obtained:

$$\tilde{M}(t) = (A - C)\, r(t)\; p(t) + E(p(t)^2 - r(t)^2) \tag{10.1}$$

and

$$\begin{bmatrix} \tilde{L}(t) \\ \tilde{N}(t) \end{bmatrix} = \begin{bmatrix} A & -E \\ -E & C \end{bmatrix} \begin{bmatrix} \dfrac{1}{\tau_p}(p_c - p(t)) \\ \dfrac{1}{\tau_r}((g/V(t))\, \sin\phi(t) - r(t)) \end{bmatrix} \tag{10.2}$$

The adopted fault tolerant structure (FTC) is displayed in Fig. 2, where $\underline{\omega}_c$ represents the target from autopilot or auto-guidance system, $\tilde{\underline{\omega}}_c$ represents the modified target taking into account the limited capability after failure, $\underline{\delta}_r$ represents the current settings for the remaining actuators, resulting from the on-line solution of the actuator reassignment problem, while $\tilde{\underline{\delta}}$ represents the effective settings of the actuators, the difference between them resulting from the actuators dynamics. The solid line represents main signal flow, and the dotted line represents the data flow for FDI function.

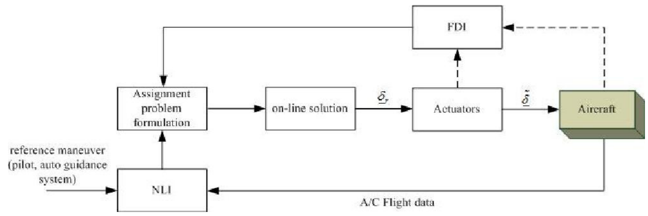

Fig. 2 Adopted Fault Tolerant Control structure

4. Formulation of Actuator Reallocation Problem

Here we consider the situations where the failure affects some of the commonly used actuators but the designed actuator redundancy still allows performing some maneuvers.

Depending on the remaining degree of redundancy between elementary actuators, it may be possible to find a solution matching exactly the following moment constraints:

$$\sum_{i\in I^L} X_i^L(t)\ \tilde{\delta}_i(t) = \tilde{L}(t) - L^0(t) \quad (11.1)$$

$$\sum_{i\in I^M} X_i^M(t)\ \tilde{\delta}_i(t) = \tilde{M}(t) - M^0(t) \quad (11.2)$$

$$\sum_{i\in I^N} X_i^N(t)\ \tilde{\delta}_i(t) = \tilde{N}(t) - N^0(t) \quad (11.3)$$

In this case the maneuver will be performed still in a standard way, otherwise, an approximate maneuver will be performed. In order to get a feasible reassignment which avoids too fast or too large solicitations of the actuators which could activate some structural modes of the aircraft, solutions as close as possible to the solution adopted at the previous control period will be privileged. Also, it is admitted that when the standard maneuver can no more be performed, a close maneuver, in fact a slightly degraded maneuver, will be retained as a running solution. So, instead of considering the pure satisfaction of the moment constraints (11.1), (11.2) and (11.3), a measure $m(\tilde{\underline{\delta}}, \tilde{L}, \tilde{M}, \tilde{N})$ of the degree of satisfaction of these constraints is introduced. In this study the following measure of satisfaction of the constraints has been adopted:

$$\begin{aligned} m(\tilde{\underline{\delta}}, \tilde{L}, \tilde{M}, \tilde{N}) = & w_L(\sum_{i\in I^L} X_i^L(t)\ \tilde{\delta}_i(t) - \tilde{L}(t) + L^0(t))^2 \\ & + w_M(\sum_{i\in I^M} X_i^M(t)\ \tilde{\delta}_i(t) - \tilde{M}(t) + M^0(t))^2 \\ & + w_N(\sum_{i\in I^N} X_i^N(t)\ \tilde{\delta}_i(t) - \tilde{N}(t) + N^0(t))^2 \end{aligned} \quad (12)$$

where w_L, w_M and w_N are positive weights. Then we formulate a linear quadratic optimization problem to be solved on-line. This problem considers the following objective function to be minimized:

$$J(\underline{\tilde{\delta}}) = \sum_{i \in I} \pi_i \cdot (\tilde{\delta}_i(t) - \tilde{\delta}_i(t-\Delta t))^2 + \gamma \cdot m(\underline{\tilde{\delta}}, \tilde{L}, \tilde{M}, \tilde{N}) \tag{13}$$

where the π_i, $i \in I$ and γ are positive weights.
The complete definition of this optimization problem is such as:

$$\min_{\underline{\tilde{\delta}}} J(\underline{\tilde{\delta}}) \tag{14}$$

with the following structural constraints:

$$A_b(t) + \sum_{i \in I^{wing}} Y_{bi}(t)\ \tilde{\delta}_i(t) \le M_{bend}^{\max} \tag{15.1}$$

$$A_f(t) + \sum_{i \in I^{wing}} Y_{fi}(t)\ \tilde{\delta}_i(t) \le M_{flex}^{\max} \tag{15.2}$$

and with the box constraints:

$$\max\left\{\delta_i^{\min}, \tilde{\delta}_i(t-\Delta t) + \dot{\delta}_i^{\min}\Delta t\right\} \le \tilde{\delta}_i(t) \le \min\left\{\delta_i^{\max}, \tilde{\delta}_i(t-\Delta t) + \dot{\delta}_i^{\max}\Delta t\right\} \quad i \in I_{\bar{F}} \tag{16.1}$$

$$\max\left\{\tilde{\delta}_i^{\min}, \tilde{\delta}_i(t-\Delta t) + \dot{\delta}_i^{\min}\Delta t\right\} \le \tilde{\delta}_i(t) \le \min\left\{\tilde{\delta}_i^{\max}, \tilde{\delta}_i(t-\Delta t) + \dot{\delta}_i^{\max}\Delta t\right\} \quad i \in I_{FL} \tag{16.2}$$

$$\max\left\{\tilde{\delta}_i^{\min}, \tilde{\delta}_i(t-\Delta t) + \dot{\tilde{\delta}}_i^{\min}\Delta t\right\} \le \tilde{\delta}_i(t) \le \min\left\{\tilde{\delta}_i^{\max}, \tilde{\delta}_i(t-\Delta t) + \dot{\tilde{\delta}}_i^{\max}\Delta t\right\} \quad i \in I_{FS} \tag{16.3}$$

with

$$\tilde{\delta}_{i_j} = 0 \ \ if\ i_j \in I_{FF},\ \ j \in \{p, q, r, ths\} \tag{17.1}$$

$$\tilde{\delta}_{i_j} = \bar{\delta}_{i_j} \ \ if\ i_j \in I_{FP},\ \ j \in \{p, q, r, ths\} \tag{17.2}$$

where $I_{\bar{F}}$ is the set of fully operational actuators, I_{FL}, I_{FS} are respectively the set of actuators whose angular positions, angular speed are subject to additional limitations, I_{FF} is the set of actuators which are not subject to a torque from their servo-control and with a zero deflection, I_{FP} is the set of actuators which are stuck at a known angular position. The positive parameters w_L, w_M and w_N are chosen in the case of a roll maneuver such as:

$$w_L >> w_M \ \ and \ \ w_L >> w_N \tag{18}$$

The above mathematical programming problem can be solved using standard programming techniques. Using the previous period value of the deflections of the actuators as initial values of current period, then in a few iterations the solution of this small size linear quadratic problem should be obtained.

5. Numerical Solvers Applied to Linear Quadratic Optimization Problems

Problem (14-17) can be rewritten as a general quadratic programming problem as follows:

$$\min_{\underline{\delta}} \ f\left(\underline{\delta}\right) = \frac{1}{2}\underline{\delta}^T Q \underline{\delta} + \underline{c}^T \underline{\delta} \tag{19}$$

$$s.t. \quad g\left(\underline{\delta}\right) = A\underline{\delta} - \underline{b} \leq \underline{0} \tag{20.1}$$

$$\underline{\xi}^- \leq \underline{\delta} \leq \underline{\xi}^+ \tag{20.2}$$

where $\underline{\delta} \in R^{n\times 1}$ is the actuator deflections vector in our case and matrix $Q \in R^{n\times n}$ is assumed to be symmetric positive definite, $A \in R^{m\times n}$, $\underline{b} \in R^{m\times 1}$. This problem, as a convex mathematical programming problem can be solved by many different iterative algorithms [13,14]. Recently, classical methods such as active set and interior point methods have been applied to the actuator allocation problem [15,16] and to fault tolerant control [8,9]. Also, dynamic solvers based on neural network have been proposed to solve the considered problem in the context of fault tolerant control [7].

Based on duality theory of Mathematical Programming and Lagrangian function, a lower bound can be found for the performance of the solution of the optimization problem (19, 20). Assume that the set of constraints (20) is not empty, otherwise there will be no possibility to perform the proposed maneuver. Then based on the first order derivative of the Lagrangian function, the complementary conditions and constraints, necessary and sufficient Karush-Kuhn-Tucker (KKT) conditions [17] can be deduced for the optimal solution of problem (19, 20) [13,14]. Then, by finding a solution satisfying the KKT conditions, the optimal solution of the original problem is obtained. Many numerical solvers such as active set, interior point and neural network are based on this idea. For convenience, we list only the basic ideas while the details of the corresponding algorithms can be found in [13,14,18].

The two main characteristics which are expected from the considered methods in this real time context are a very short computation time with respect to the response time of the actuators (a ratio around one to ten) and the feasibility of the solution even in a time-out situation in which the optimization process is interrupted.

5.1. Active Set Methods

Active set is a name for a family of methods used to solve optimization problems with a relatively large number of interval constraints. The idea underlying active set methods is to generate successive partitions of the inequality constraints set into two groups: one where the constraints are to be treated as active constraints and one where the constraints are to be treated as inactive constraints (and be ignored someway at a given stage of the solution process). At each iteration, active inequality constraints will be treated as equality ones and constitute the working set. Through the partitions of the inequality constraints set, the method reduces the constrained problem to a sequence of equality constrained sub-problems where the inactive ones are temporarily ignored, while an updating process modify the working set along the search process towards the solution.

Problem (19, 20) can be written as:

$$\min_{\underline{\delta}} \ f\left(\underline{\delta}\right) = \frac{1}{2}\underline{\delta}^T Q \underline{\delta} + \underline{c}^T \underline{\delta} \tag{21}$$

$$s.t. \quad g\left(\underline{\delta}\right) = \tilde{A}\underline{\delta} - \underline{\tilde{b}} \leq \underline{0} \tag{22}$$

where $\tilde{A} = \begin{bmatrix} A^T & I_d^T & -I_d^T \end{bmatrix}^T$, $\underline{\tilde{b}} = \begin{bmatrix} \underline{b}^T & \underline{\xi}^{+T} & -\underline{\xi}^{-T} \end{bmatrix}^T$ and I_d is an identity matrix of size $n\times n$.

At each iteration, the active set method solves a sub-problem (equality constrained QP) written as:

$$\min_{\underline{\delta}} \; f_w\left(\underline{\delta}\right) = \frac{1}{2}\underline{\delta}^T Q \underline{\delta} + \underline{c}^T \underline{\delta} \tag{23}$$

$$s.t. \quad \tilde{A}_w \underline{\delta} - \underline{\tilde{b}}_w = \underline{0} \tag{24}$$

The subscript w denotes the working set index. The solution at the k^{th} iteration is written $\underline{\delta}_k$. Let $\underline{p}_{k+1}$ be the solution of problem (23, 24) at iteration k. Then we have:

$$\min_{\underline{p}_{k+1}} \; f_w\left(\underline{p}_{k+1}\right) = \frac{1}{2}\underline{p}_{k+1}^T Q \underline{p}_{k+1} + \underline{p}_{k+1}^T\left(Q\underline{\delta}_k + \underline{c}\right) \tag{25}$$

$$s.t. \quad \tilde{A}_w \underline{p}_{k+1} = \underline{0} \tag{26}$$

Consider the KKT conditions of problem (25, 26).

$$\begin{bmatrix} Q & \tilde{A}_w^T \\ \tilde{A}_w & 0 \end{bmatrix} \begin{Bmatrix} \underline{p}_{k+1} \\ \underline{\lambda}_{k+1} \end{Bmatrix} = \begin{Bmatrix} -\left(Q\underline{\delta}_k + \underline{c}\right) \\ \underline{0} \end{Bmatrix} \tag{27}$$

As long as $\tilde{A}_w$ is full row-rank, and since Q is here a positive definite matrix, the coefficient matrix in (27) termed as KKT matrix is nonsingular [14]. Then Solving (27) is straightforward and we obtain a new search direction $\underline{p}_{k+1}$ and the associated Lagrange multipliers $\underline{\lambda}_{k+1}$. According to their values, the current solution may be an optimum or else it should be updated.

When the current solution needs to be updated, the corresponding step length can be derived from a line search process:

$$\underline{\delta}_{k+1} = \underline{\delta}_k + \alpha_{k+1}\underline{p}_{k+1} \tag{28}$$

To make sure that $\underline{\delta}_{k+1}$ is feasible, it is only necessary to consider the constraints that are not in the working set and such as $\tilde{A}_i \underline{p}_{k+1} > 0$, while α_{k+1} must be as large as possible within [0,1]. So α_{k+1} is given by:

$$\alpha_{k+1} = \min\left\{1, \min_{i \notin w_k, \tilde{A}_i \underline{p}_{k+1} > 0}\left(\frac{\tilde{b}_i - \tilde{A}_i \underline{\delta}_k}{\tilde{A}_i \underline{p}_{k+1}}\right)\right\} \tag{29}$$

Based on the above considerations, an algorithm can be derived. For the details of the algorithm, see [8]. If there are only bound constraints and no other inequality constraints, problem (25, 26) can be reformulated as an unconstrained least square problem like in [15] and the computation of its solution will be easier. In the present case, with the presence of structural integrity constraints, the method based on the KKT matrix should be used.

It has been already proved that the active set method solves problems such as (19, 20) after a rather small number of iterations [13].

5.2. Interior Point Methods

The idea of interior point methods is to approach the solution of the KKT equations by successive descent steps. Each descent step is a Newton-like step and is obtained by solving a system of linear equations. The main advantage of interior point methods over active set method is their scalability [16,19].

To turn problem (19, 20) into a standard form for interior point methods, let

$$\underline{\delta} = \underline{x} + \underline{\xi}^{-} \tag{30}$$

Substituting (30) into (19) and (20), and omitting the constant term in the objective function which will not impact the final solution, the original problem is equivalent to the following problem:

$$\min_{\underline{x}} \; f(\underline{x}) = \frac{1}{2}\underline{x}^T Q \underline{x} + \underline{x}^T \underline{\tilde{c}} \tag{31}$$

$$s.t. \quad g(\underline{x}) = A\underline{x} + \underline{\tilde{b}} \le \underline{0} \tag{32.1}$$

$$\underline{0} \le \underline{x} \le \underline{x}^{+} \tag{32.2}$$

where $\underline{\tilde{c}} = Q\xi^{-} + \underline{c}$, $\underline{\tilde{b}} = A\xi^{-} - \underline{b}$ and $\underline{x}^{+} = \xi^{+} - \xi^{-}$.
Adding slack variables $\underline{y}$, $\underline{z}$ to turn inequalities into equalities, we get the following formulation:

$$\min_{\underline{x}} \; \frac{1}{2}\underline{x}^T Q \underline{x} + \underline{x}^T \underline{\tilde{c}} \tag{33}$$

$$s.t. \quad A\underline{x} + \underline{\tilde{b}} + \underline{y} = \underline{0}, \quad \underline{x} + \underline{z} = \underline{x}^{+} \tag{34.1}$$

$$\underline{x} \ge \underline{0}, \underline{y} \ge \underline{0}, \underline{z} \ge \underline{0} \tag{34.2}$$

One of the basic ideas behind the interior point methods is to use barrier functions to satisfy the bound constraints. Then a modified Lagrangian for problem (33, 34) expressed as:

$$\begin{aligned} L= & \frac{1}{2}\underline{x}^T Q \underline{x} + \underline{x}^T \underline{\tilde{c}} - \tau\sum_{i=1}^{n}\log(x_i) - \tau\sum_{i=1}^{m}\log(y_i) \\ & -\tau\sum_{i=1}^{n}\log(z_i) + \underline{\mu}^T\left(A\underline{x} + \underline{\tilde{b}} + \underline{y}\right) + \underline{\varphi}^T\left(\underline{x} + \underline{z} - \underline{x}^{+}\right) \end{aligned} \tag{35}$$

is introduced, where $\tau > 0$ is the barrier parameter and is used to guide the solution along a trajectory called the *central path*. Equation (35) approximates the Lagrangian of problem (33, 34) more and more closely as τ goes to zero [13,14]. Here $\underline{\mu}$, $\underline{\varphi}$ are the dual variables associated to the equality constraints (34.1). Adopting the modified Lagrangian function (35), the necessary and sufficient conditions for the global minimum of convex problem (35) i.e. the KKT conditions, can be derived as:

$$\nabla_{\underline{x}} L = Q\underline{x} + \underline{\tilde{c}} - \underline{\lambda} + A^T\underline{\mu} + \underline{\varphi} = \underline{0} \tag{36.1}$$

$$\nabla_{\underline{y}} L = Y\underline{\mu} - \tau\underline{e} = \underline{0} \tag{36.2}$$

$$\nabla_{\underline{z}} L = Z\underline{\varphi} - \tau\underline{e} = \underline{0} \tag{36.3}$$

$$X\underline{\lambda} - \tau\underline{e} = \underline{0} \tag{36.4}$$

$$\nabla_{\underline{\mu}} L = A\underline{x} + \underline{\tilde{b}} + \underline{y} = \underline{0} \tag{36.5}$$

$$\nabla_{\underline{\varphi}} L = \underline{x} + \underline{z} - \underline{x}^{+} = \underline{0} \tag{36.6}$$

$$\underline{x} > \underline{0}, \underline{y} > \underline{0}, \underline{z} > \underline{0}, \underline{\lambda} > \underline{0}, \underline{\mu} > \underline{0}, \underline{\varphi} > \underline{0} \quad (36.7)$$

where X, Y, and Z are diagonal matrices whose diagonal elements are $\underline{x}$, $\underline{y}$, $\underline{z}$ respectively. Here $\underline{\lambda}$ is another dual variable. The quantity $\underline{x}^T\underline{\lambda} + y^T\underline{\mu} + \underline{z}^T\varphi$ is termed as *duality ga*p [13,14].

Applying Newton's method to the above system of equations (36), we obtain the linear system to be solved:

$$\begin{bmatrix} Q & 0 & 0 & -I_{d1} & A^T & I_{d1} \\ 0 & \mathrm{M} & 0 & 0 & Y & 0 \\ 0 & 0 & \Phi & 0 & 0 & Z \\ \Lambda & 0 & 0 & X & 0 & 0 \\ A & I_{d2} & 0 & 0 & 0 & 0 \\ I_{d1} & 0 & I_{d1} & 0 & 0 & 0 \end{bmatrix} \begin{Bmatrix} \Delta\underline{x} \\ \Delta\underline{y} \\ \Delta\underline{z} \\ \Delta\underline{\lambda} \\ \Delta\underline{\mu} \\ \Delta\underline{\varphi} \end{Bmatrix} = -\begin{Bmatrix} \underline{r}_x \\ \underline{r}_y \\ \underline{r}_z \\ \underline{r}_\lambda \\ \underline{r}_\mu \\ \underline{r}_\varphi \end{Bmatrix} \quad (37)$$

where Λ, M and Φ are diagonal matrices whose diagonal elements are $\underline{\lambda}$, $\underline{\mu}$ and $\underline{\varphi}$, respectively. The $I_{d\cdot}$ matrices are identity matrices with appropriate dimensions. The residuals $\underline{r}_\cdot$ are defined as:

$$\begin{aligned} &\underline{r}_x = Q\underline{x} + \underline{\tilde{c}} - \underline{\lambda} + A^T\underline{\mu} + \underline{\varphi},\ \ \underline{r}_y = Y\underline{\mu} - \tau\underline{e},\ \ \underline{r}_z = Z\underline{\varphi} - \tau\underline{e}, \\ &\underline{r}_\lambda = X\underline{\lambda} - \tau\underline{e},\ \ \underline{r}_\mu = A\underline{x} + \underline{\tilde{b}} + \underline{y},\ \ \underline{r}_\varphi = \underline{x} + \underline{z} - \underline{x}^+ \end{aligned} \quad (38)$$

Equation (38) can be solved progressively as:

$$\begin{aligned} &\Delta\underline{x} = -H^{-1}\underline{r}_t,\ \Delta\underline{y} = -\left(\underline{r}_\mu + A\Delta\underline{x}\right),\ \Delta\underline{z} = -\left(\underline{r}_\varphi + \Delta\underline{x}\right), \\ &\Delta\underline{\lambda} = -X^{-1}\left(\underline{r}_\lambda + \Lambda\Delta\underline{x}\right),\ \Delta\underline{\mu} = -Y^{-1}\left(\underline{r}_y + \mathrm{M}\Delta\underline{y}\right), \\ &\Delta\underline{\varphi} = -Z^{-1}\left(\underline{r}_z + \Phi\Delta\underline{z}\right) \end{aligned} \quad (39.1)$$

where

$$H = Q + X^{-1}\Lambda + A^TY^{-1}\mathrm{M}A + Z^{-1}\Phi \quad (39.2)$$

$$\underline{r}_t = \underline{r}_x - A^TY^{-1}\underline{r}_y - Z^{-1}\underline{r}_z + X^{-1}\underline{r}_\lambda + A^TY^{-1}\mathrm{M}\underline{r}_\mu + Z^{-1}\Phi\underline{r}_\varphi \quad (39.3)$$

Since Q is positive definite, A is full row rank and during iteration, $\underline{x}$, $\underline{y}$, $\underline{z}$, $\underline{\lambda}$, $\underline{\mu}$, $\underline{\varphi}$ remain greater than zero, H is an invertible matrix.

Various algorithms can be derived depending on whether solving the primal or the dual variables and on the choice of the initial point $\underline{x}^0$. Following [16], the values of $\underline{x}^0$, $\underline{z}^0$, $\underline{\lambda}^0$, $\underline{\mu}^0$, $\underline{\varphi}^0$ can be chosen such that $\underline{r}_x$=0 and $\underline{r}_\varphi$=0. In the present case, $\underline{x}^0$ may be chosen as the vector of the mean values of the upper and lower bounds or the values at the previous instant. Then, the values of $\underline{z}^0$, $\underline{\lambda}^0$, $\underline{\mu}^0$, $\underline{\varphi}^0$ are chosen based on the values of $\underline{x}^0$. Moreover, under normal situation, (34.1) can be strictly satisfied with a positive vector $\underline{y}^0$ and $\underline{z}^0$.

Based on (38, 39), a feasible-initialization primal-dual path-following algorithm has been be proposed in [9] where the detailed description and setting of the method are available. It appeared there that interior point methods can handle the considered failure situation satisfactory even if some realistic factors such as the dynamics of the actuators and dynamic inversion controller time lags have not been considered in the problem formulation.

5.3. Neural Network Method

The basic idea for solving an optimization problem using a tailored neural network is to make sure that the neural network will converge asymptotically and that the equilibrium point of the neural network will correspond to the optimal solution of the optimization problem. Motived by the online solution of linear and quadratic programs, a primal-dual neural network scheme based on linear variational inequalities (LVI) has been proposed by Zhang which has proven its global convergence [18] Based on the KKT conditions of problem (19, 20), the original problem can be turned equivalent to the following set of linear variational inequalities:

$$\left(\underline{s}-\underline{s}^*\right)^T\left(N\underline{s}^*+\underline{p}\right)\geq 0 \quad \forall \underline{s}\in\Omega \tag{40}$$

with the primal-dual variables $\underline{s}=[\,\underline{\delta}^T \;\; \underline{u}^T]^T$, $\underline{u}$ is the dual variable vector corresponding to inequality constraint (20.1). Then the problem is to find a solution vector $\underline{s}^*$ where its feasible region Ω and its lower/ upper limits are given by:

$$\Omega := \left\{\underline{s}\,\middle|\,\underline{\varsigma}^- \leq \underline{s} \leq \underline{\varsigma}^+\right\}, \underline{\varsigma}^- = \left[\underline{\xi}^- \quad \underline{0}\right]^T, \underline{\varsigma}^+ = \left[\underline{\xi}^+ \quad \underline{\omega}^+\right]^T \tag{41}$$

Here $\underline{\omega}^+$ is considered with the appropriate dimension and each of its entries is sufficiently large to replace numerically $+\infty$. The coefficients are defined as:

$$\underline{\rho} = \left[\underline{c}^T \quad \underline{b}^T\right]^T \quad N = \begin{bmatrix} Q & A^T \\ -A & 0 \end{bmatrix} \tag{42}$$

Then the neural network model which solves problem (19, 20) is given by:

$$\frac{d\underline{s}}{dt} = \eta\left(I_{d3}+N^T\right)\left\{P_\Omega\left(\underline{s}-\left(N\underline{s}+\underline{\rho}\right)\right)-\underline{s}\right\} \tag{43}$$

where η is a positive learning parameter which can be used to adjust the convergence speed of the network, I_{d3} is an identity matrix, $P_\Omega[\cdot]$ is a piecewise-linear function defined as:

$$P_\Omega\left[s_i\right] = \begin{cases} \varsigma_i^-, & \text{if } s_i \leq \varsigma_i^- \\ \varsigma_i^+, & \text{if } s_i \geq \varsigma_i^+ \\ s_i, & \text{otherwise} \end{cases} \tag{44}$$

Numerical application of this neural network approach have shown its feasibility [7].

6. Comparative Application of the Three Solvers to the Actuators Reassignment Problem

Here we consider a large transport aircraft with 120 tons, flight speed 120m/s, initial angle of attack is 4º, the desired maneuver is a coordinated turn expressed in (9). This aircraft has four ailerons, four elevators, and two rudders whose position and slew rate limits are given in Table 1. All these actuators follow first-order dynamics and their time constants are also shown in Table 1. The time constant in (9) are all chosen as 1/3s. The adopted control scheme is illustrated as Fig. 2. Here mainly give the simulation results of the optimized based control allocation problem (19), (20). Due to the lack of modeling parameters, structural constraints are not considered. Actually, with the command governor, it will not affect the demonstration because there always exists solutions to the problem.

Table 1. Parameters of actuators under nominal condition

Actuator	No. of actuators	Position limits	Slew rate limits	Time constant
aileron	4	-25º ~ 25º	-25º/s ~ 25º/s	0.15s
elevator	4	-25º ~ 10º	-15º/s ~ 15º/s	0.15s
rudder	2	-30º ~ 30º	-25º/s ~ 25º/s	0.3s

To check the feasibility and performances of three solvers for on-line flight fault tolerant control, two fault scenarios have been considered: a soft one where only a deflection rate is affected by a fault and a hard one where a main actuator remains stuck. The command and desired coordinated maneuver to be performed is illustrated in Fig. 3 where only roll rate is illustrated and pitch must maintained equal to zero, and yaw rate will change according to equation (9.3). We hope the final maneuver will be as closely as possible to the desired maneuver. From Fig. 3 to Fig. 13, the star symbol denotes the failure instant.

In the numerical application, the sampling time adopted by the digital control system of the different actuators is taken equal to 0.05s. The weights of the optimality criterion (13) are chosen as, $\gamma = 10^{-6}$, the weighting parameters for various angle rates and actuators are all equal to one. The parameters for the neural network are chosen as 10^{10} to replace numerically $+\infty$ in (41) and $\eta = 10^7$.

6.1. Soft Fault Scenario

In this case it is assumed that all actuators are fault free except for the rate limits of the right outer aileron which changes to ± 5 deg/s at 1s.

The time evolution of ailerons command is shown in Fig. 4 where smooth evolutions can be observed and the trajectory are only small different for three solvers. From Fig. 5 (a) and (b), active set method appears to need much less iterations than the programmed interior point method because of the small size of the problem (the computation time is not accurate because it changes a lot between different run). Also, the whole convergence trajectory of the built neural network for different instant is shown in Fig. 6 (a), which seems like a staircase because of the fast convergence at each instant and it takes about 0.01ms to convergent as shown in Fig. 6 (b). Under these three methods, desired maneuver will be almost obtained from Fig. 7 (a) to (c), the differences between real and desired maneuver mainly from the actuator dynamics. Fig. 8 (a), (b) and (c) display the speed of the failed actuator which reaches at different stages its speed limit when using active set and neural network and the trajectory look the same under these two solvers, however, it never reaches speed limit when using interior point due to the contour of objective function become very smooth and not enough iteration has been done for interior point. From them, it seems that the performance of active set method is the best because it will find the exact optimum at a fast speed, and the performance of neural network is almost the same as active set. It appears that these three methods can handle the soft failure situation satisfactory even if many realistic factors such as time lags caused by FDI and NLI are not considered.

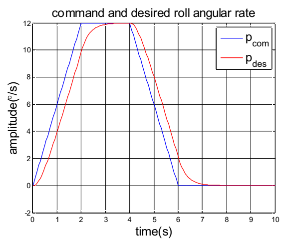

Fig. 3 Time evolution of command and desired maneuver (only display roll angular rate, pitch and yaw rates remain at zeros)

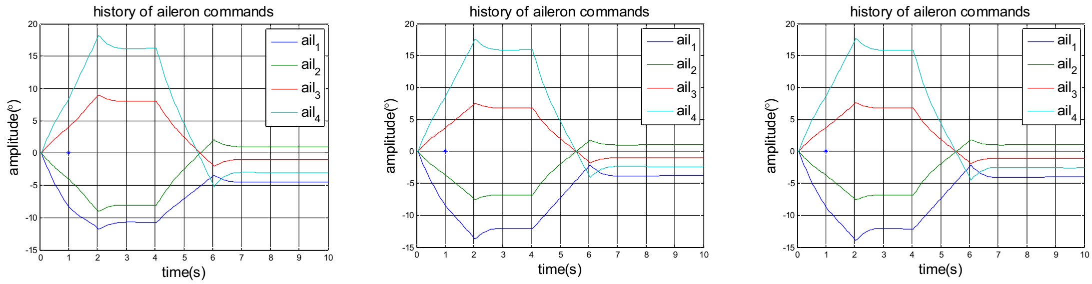

(a) Result of interior point; (b) Result of active set; (c) Result of neural network

Fig. 4 Evolution of ailerons commands under soft fault scenario

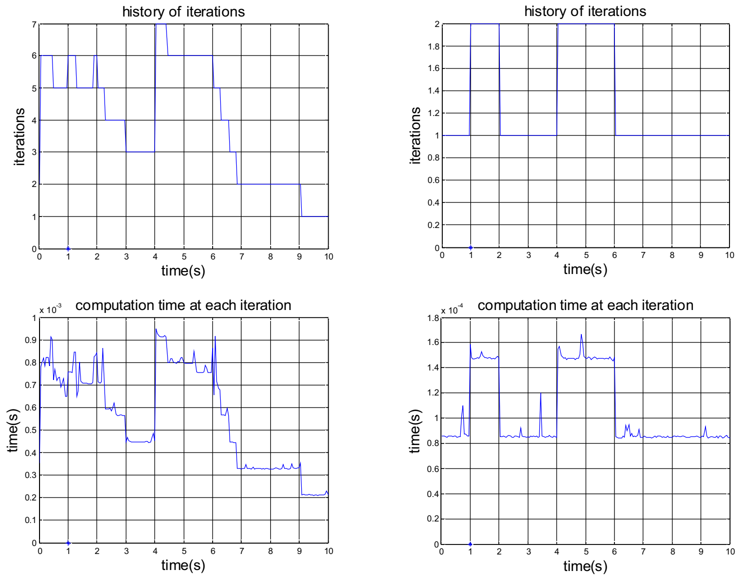

(a) Result of interior point; (b) Result of active set

Fig. 5 Number of iterations and computation time for interior point and active set under soft fault scenario

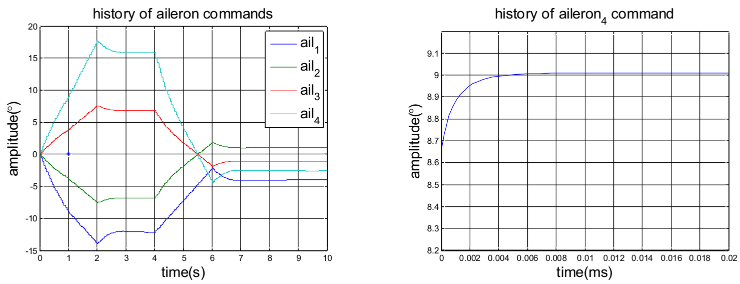

(a) Evolution of network outputs during the whole time-span; (b) zoomed picture to show the convergence speed of network

Fig. 6 Convergent behavior of the neural network solver (0.01ms)

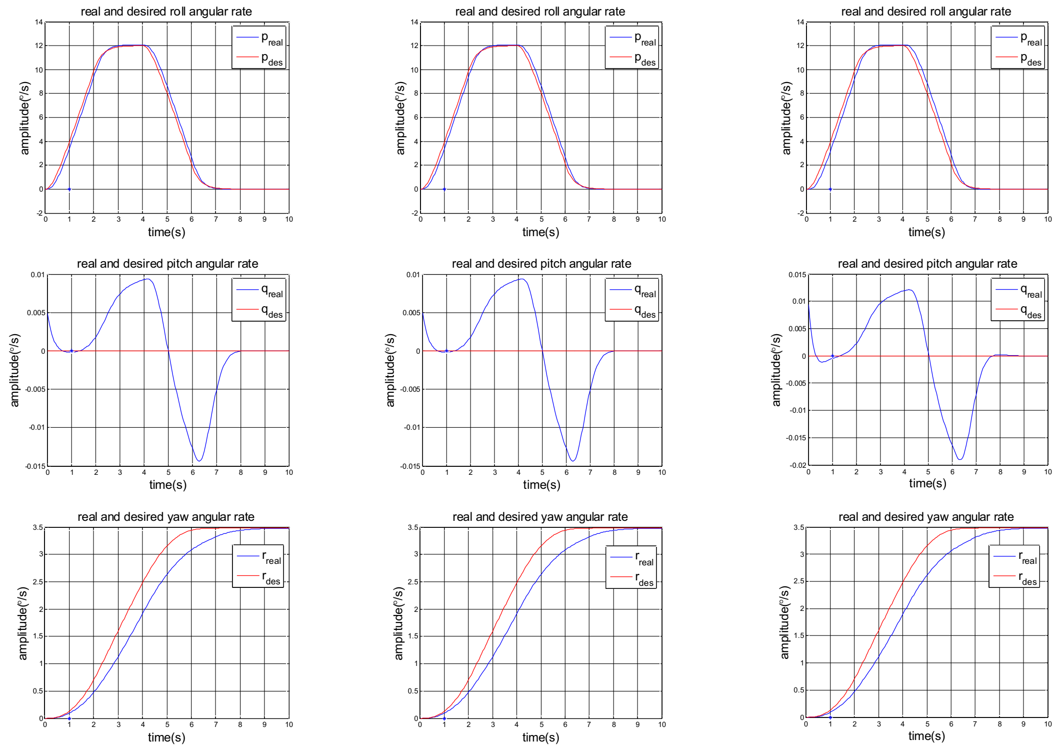

(a) Result of interior point; (b) Result of active set; (c) Result of neural network

Fig. 7 The real and desired angular rates under soft fault scenario

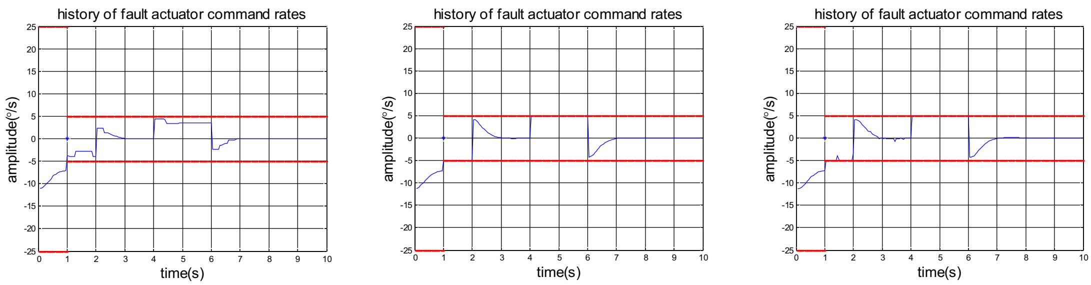

(a) Result of interior point; (b) Result of active set; (c) Result of neural network

Fig. 8 Command rates for the right outer aileron under soft fault scenario

6.2. Hard Fault Scenario

A more serious failure case occurs when an actuator remains stuck. Here, while the configuration of the neural network remains the same, since a box constraint is considered by the interior point algorithm and for the simplicity of the problem, the column corresponding to the stuck actuator must be deleted from the control effectiveness matrix and the virtual control input and limits should be changed accordingly under interior point and active set methods.

We simulate the case where the right outer aileron is stuck at its current position at 1s. Simulation parameters are the same as before. The corresponding results are displayed from Fig. 9 to Fig. 13.

Here again since angular dynamics, actuator deflections and speed are small different with the three techniques, they are displayed in Fig. 9, Fig. 10 and Fig. 13. From Fig. 9 and Fig.13, it can be concluded that in the considered case, the three methods achieve to deal effectively with the faulty actuator stuck at a fixed position.

From Fig. 10 (a) and (b), it also appears that the active set method needs less iterations than the interior point method may be because of the small size of the problem. It is maybe due to the same reason when compare Fig. 5 (b) and Fig. 10(b). Here also, the neural network converges to the solution in 0.01 ms as shown in Fig. 12. From Fig. 13 (a), (b) and (c), we notice that for three methods, a downgraded maneuver is obtained. There is a constant deviation for roll rate as shown in Fig. 10, it is because the actuator command consider in the optimal problem is different from the actual actuator position and cause a constant deviation in the final angular rate. This deviation also exists in yaw rate but it is less the deviation in pitch angular rate.

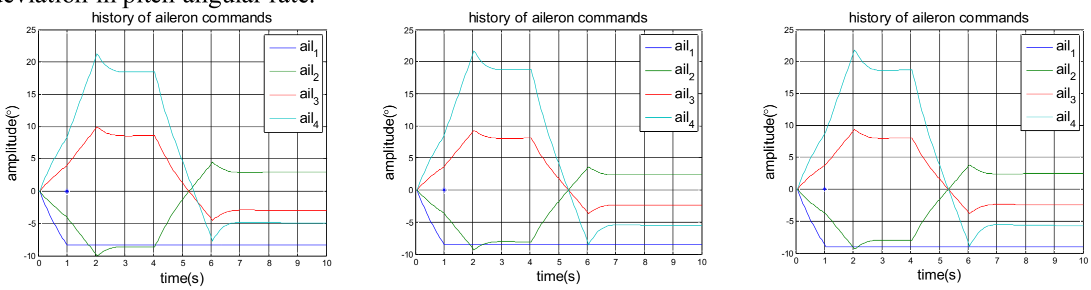

(a) Result of interior point; (b) Result of active set; (c) Result of neural network

Fig. 9 Evolution of actuators commands under hard fault scenario

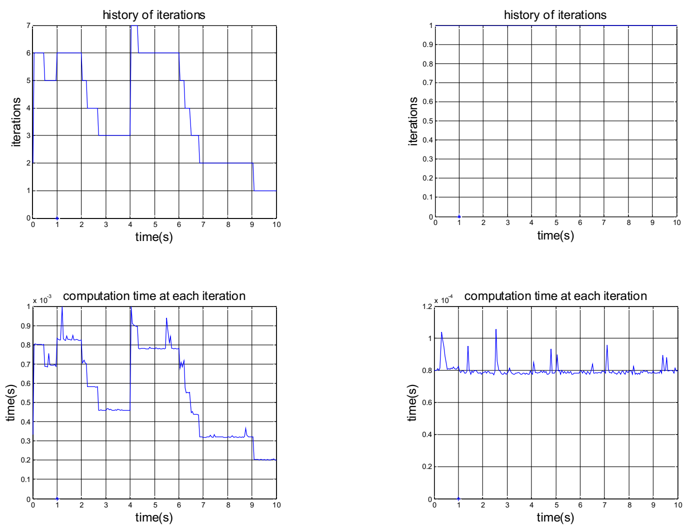

(a) Result of interior point; (b) Result of active set

Fig. 10 Number of iterations and computation time for interior point and active set under hard fault scenario

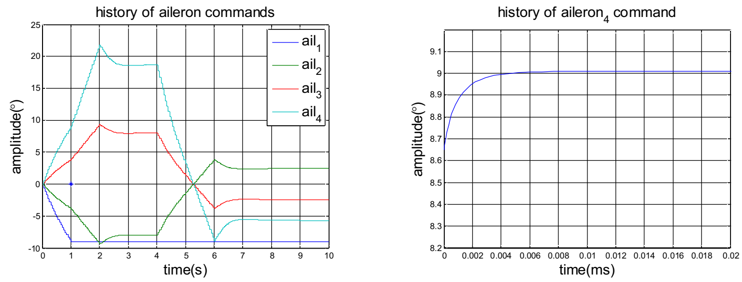

(a) Evolution of network outputs during the whole time-span;

(b) zoomed picture to show the convergence speed of network

Fig. 11 Convergent behavior of the neural network solver (0.01ms)

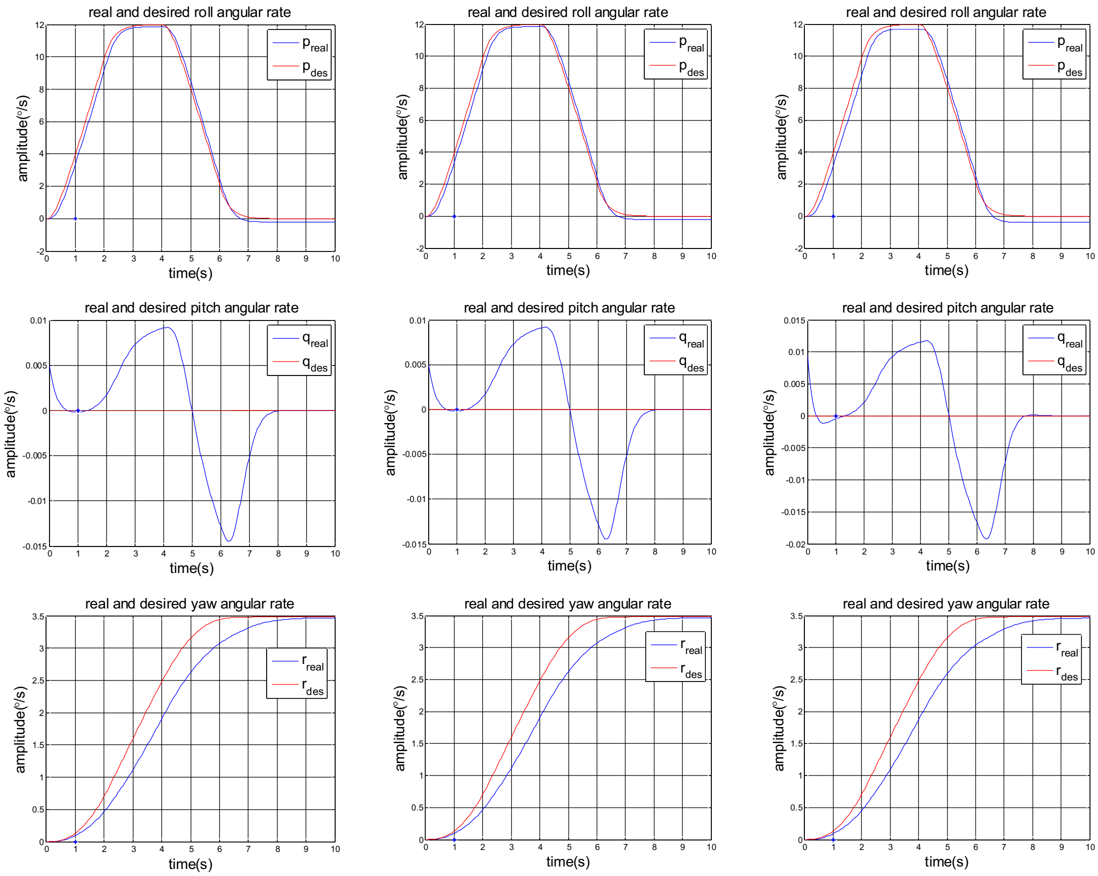

(a) Result of interior point;

(b) Result of active set;

(c) Result of neural network

Fig. 12 The real and desired angular rates under hard fault scenario

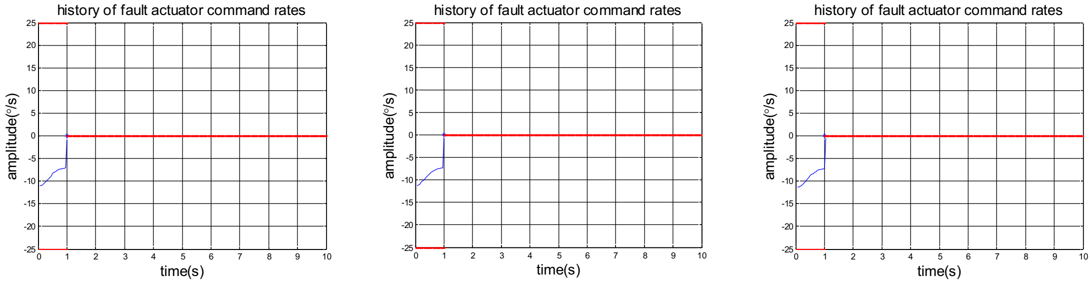

(a) Result of interior point; (b) Result of active set; (c) Result of neural network

Fig. 13 Command rates for the right outer aileron under hard fault scenario

From the simulation results above, it appears that the three considered methods are able, for the two failure scenarios, to provide the optimal solution with an acceptable response time. The neural network method presents by far the best performance with respect to computation time (at most 0.01 ms to compare with a common actuator sampling time of 0.05s) but feasibility of the solution is only guaranteed at convergence. The computation time performance of the active set method is a little bit better than the one of the interior point method, both being acceptable. Also these two methods provide at each step a feasible solution which can be adopted in the case of time-outs. The interior point method reaches the solution after a larger number of iterations than the active set method but it copes with a problem of larger dimensions (more variables and more constraints). From the point of view of algorithmic complexity, the active set method presents the lower complexity and when an actuator failure is detected and identified, the setting of the resulting optimization problem and solver appears easier than for the interior point method. In the case of the neural network solver, its structure is already fixed and some parameters will be changed according to the result of the FDI process.

7. Conclusion

In this study the control surface reassignment and resetting when a transport aircraft encounter one major actuator failure has been considered. The main objective is here to guarantee the flight safety through the consideration of the remaining maneuverability of the faulty aircraft and maintaining as much as possible the capability of the aircraft to achieve in a nominal way the necessary maneuvers to follow a flight plan. Structural constraints are also taken into account. So, it has been shown how to obtain the desired maneuver on the basis of a perfect non linear inversion of the flight dynamics.

Numerical methods such as the active set method, the interior point method and a solver based on dynamic neural networks techniques, have been analyzed and applied to this optimization problem. In both considered actuator failure scenarios (soft and hard actuator failure), the three solution approaches have demonstrated interesting performances with some preference for the active set method. Anyway, the results obtained from the application of these solution methods demonstrate clearly the feasibility of the proposed approach characterized by the on-line resolution of an optimization problem.

References

[1] Napolitano MR, Casdorph V, Neppach C, Naylor S. On-line learning neural architectures and cross-correlation analysis for actuator failure detection and identification. *International Journal of Control* 1996; 63(3): 433-455.

[2] Hwang, I., Kim, S., Kim, Y., and Seah, C. E. A Survey of Fault Detection, Isolation, and Reconfiguration Methods. *IEEE Transactions on Control Systems Technology* 2010; 18(3): 636-653.

[3] Han, Y., Oh, S., Choi, B., Kwak, D., Kim, H. J., and Kim, Y. Fault detection and identification of aircraft control surface using adaptive observer and input bias estimator. *IET Control Theory & Applications*, 2012; 6(10): 1367-1387.

[4] España, M. and Gilyard, G. Aircraft Adaptive Performance Optimization Using Redundant Control Effectors. *Automatic Control in Aerospace*, Palo Alto, CA USA, 1994, p. 12-16.

[5] Gaulocher, S. L., Cumer, C. and Alazard, D. Aircraft load alleviation during maneuvers using optimal control surface combinations. *Journal of Guidance Control and Dynamics* 2007; 30(2): 591-600.

[6] Burken, J. J., Lu, P., Wu, Z. and Bahm, C. Two Reconfiguration Flight-Control Design Methods: Robust Servomechanism and Control Allocation. *Journal of Guidance, Control and Dynamics* 2001; 24(3): 482-494.

[7] Zhong, L., Mora-Camino, F. Neural Networks Based Aircraft Fault Tolerant Control. *14th AIAA/ISSMO Conference*, Indiana, USA, 2012.

[8] Zhong, L., Mora-Camino, F. Aircraft Fault Tolerant Control Based on Active Set Method. *25th Chinese Control and Decision Conference,* Guiyang, China, 2013.

[9] Zhong, L., Mora-Camino, F. Aircraft Fault Tolerant Control Based on Interior Point Method. 32nd Chinese Control Conference, Xi'an, China, 2013 (accepted).

[10] Etkin, B. and Reid, L. D., *Dynamics of flight: stability and control*, 3rd edition, Wiley; 1995.

[11] Roux, E. *Modèle de Masse Voilure: Avions de transport civil*. Ph.D. Dissertation, SupAéro-ONERA, Toulouse, France, 2006.

[12] Andrei,G. *Contribution à la commande tolérante aux pannes pour la conduite du vol*. Ph.D. Dissertation, INSA, Toulouse, France, 2010

[13] Luenberger, D. G. and Ye, Y., *Linear and Nonlinear Programming*. Springer, 2008.

[14] Stephen, B., Lieven, V., *Convex Optimizatio*n, Cambridge University Press, 2004.

[15] Harkegard, O. Efficient active set algorithms for solving constrained least squares problems in aircraft control allocation. *41st IEEE Conference on Decision and Control*, Las Vegas, NV, USA; 2002, p. 1295-1300.

[16] Peterson J.A.M. and Bodson, M. Interior-point Algorithms for Control Allocation. *Journal of guidance, control, and dynamics* 2005; 28(3): 471-480.

[17] Kuhn, H. W., Tucker, A. W. Nonlinear programming. *Proceedings of 2nd Berkeley Symposium*, Berkeley; 1951, p. 481–92.

[18] Zhang, Y. On the LVI-based Primal-Dual Neural Network for Solving Online Linear and Quadratic Programming Problems. *American Control Conference*, Porland, OR, USA, 2005; p. 1351-1356.

[19] Lau, M. S. K., Yue, S. P. K., Ling, V. and Maciejowski, J. M. A Comparison of Interior Point and Active Set Methods for FPGA Implementation of Model Predictive Control. *European Control Conference*, Budapest, Hungary, 2009; p. 156-161.